sidered as potential major contributors to polar ozone loss even in years without significant volcanic eruptions.

REFERENCES AND NOTES

1. R. P. Turco and P. Hamill, *Ber. Bunsenges. Phys. Chem.* **96**, 323 (1992).
2. E. W. Wolff and R. Mulvaney, *Geophys. Res. Lett.* **18**, 1007 (1991).
3. D. R. Hanson and A. R. Ravishankara, *J. Geophys. Res.* **96**, 17307 (1991).
4. B. P. Luo, Th. Peter, P. J. Crutzen, *Ber. Bunsenges. Phys. Chem.* **96**, 334 (1992).
5. E. J. Jensen, O. B. Toon, P. Hamill, *Geophys. Res. Lett.* **18**, 1857 (1991).
6. M. A. Tolbert, M. J. Rossi, D. M. Golden, *ibid.* **15**, 847 (1988).
7. L. R. Watson *et al.*, *J. Geophys. Res.* **95**, 5631 (1990).
8. C. M. Reihs *et al.*, *ibid.*, p. 16545.
9. Equation 2 parallels the approach taken in laboratory studies when the gas uptake is dominated by solubility. In the atmosphere, the contact time between the gas and particles is long enough for the entire particle to be in equilibrium with the gas, so the liquid phase diffusion coefficient is not needed.
10. F. P. J. Valero and P. Pilewskie, *Geophys. Res. Lett.* **19**, 163 (1992).
11. In situ particle size measurements from the DC-8 at 34.6°W yielded a surface area between 10 and 13 $\mu m^2\ cm^{-3}$, which is consistent with the optical depth measurement of surface area, given the vertical variations observed by the lidar.
12. The eruption of Pinatubo occurred about 7 months before our observations. However, the column concentrations of HCl, HNO_3, and $ClNO_3$ that we observed outside the Arctic vortex in 1992 were similar to those observed in earlier nonvolcanic years, when the steadily rising amount of chlorine in the stratosphere is taken into account (*15*). Thus, the volcanic cloud had not measurably altered the concentrations of these species in extra-vortex air before the event of 19 January 1992.
13. H. Steele and P. Hamill, *J. Aerosol Sci.* **12**, 517 (1981).
14. We divided the volcanic layer into five vertical intervals spanning potential temperatures from 370 to 470 K. Trajectories were done for each of these layers. Because the aircraft location differs from that of the column chemistry measurements, trajectories were also computed for 2° latitude south of the aircraft location. The exposure times (Fig. 3) are vertical and horizontal averages of the times during which *W* was less than 60%. Exposure times at the two latitudes were within 10% of each other.
15. G. C. Toon, C. B. Farmer, P. W. Schaper, L. L. Lowes, R. H. Norton, *J. Geophys. Res.* **97**, 7939 (1992); G. C. Toon *et al.*, *ibid.*, p. 7963.
16. O. B. Toon, E. V. Browell, S. Kinne, J. Jordan, *Geophys. Res. Lett. 17*, 393 (1990).
17. R. Zhang, P. J. Wooldridge, M. Molina, *J. Phys. Chem.*, in press. Table 1 contains laboratory H^* values computed with the use of binary sulfuric acid solutions. We also computed H^*, accounting for ternary solution effects by using our measured *x* values to constrain the vapor pressures. The ternary H^* differed from the binary H^* by only about 30%.
18. R. L. Jones, D. S. McKenna, L. R. Poole, S. Solomon, *Geophys. Res. Lett.* **17**, 545 (1990).
19. J. D. Burley and H. S. Johnston, *ibid.* **19**, 1363 (1992); M. A. Tolbert, *NASA Ref. Publ.* **1293**, 50 (1993); C. A. Cantrell, J. A. Davidson, R. E. Shetter, B. A. Anderson, *J. Phys. Chem.* **41**, 6017 (1987).

20. We thank R. P. Turco, M. Coffey, and two referees for helpful comments on the manuscript, as well as the DC-8 flight crew for their hard work and dedication.

21 December 1992; accepted 13 July 1993

In Situ Observations of Aerosol and Chlorine Monoxide After the 1991 Eruption of Mount Pinatubo: Effect of Reactions on Sulfate Aerosol

J. C. Wilson,* H. H. Jonsson, C. A. Brock, D. W. Toohey, L. M. Avallone, D. Baumgardner, J. E. Dye, L. R. Poole, D. C. Woods, R. J. DeCoursey, M. Osborn, M. C. Pitts, K. K. Kelly, K. R. Chan, G. V. Ferry, M. Loewenstein, J. R. Podolske, A. Weaver

Highly resolved aerosol size distributions measured from high-altitude aircraft can be used to describe the effect of the 1991 eruption of Mount Pinatubo on the stratospheric aerosol. In some air masses, aerosol mass mixing ratios increased by factors exceeding 100 and aerosol surface area concentrations increased by factors of 30 or more. Increases in aerosol surface area concentration were accompanied by increases in chlorine monoxide at mid-latitudes when confounding factors were controlled. This observation supports the assertion that reactions occurring on the aerosol can increase the fraction of stratospheric chlorine that occurs in ozone-destroying forms.

We have made in situ observations of changes in the size distribution of stratospheric aerosols after the 15 June 1991 eruption of Mount Pinatubo. We compared these measurements with satellite and lidar measurements, which served to locate the in situ observations with respect to the vertical extent of the volcanic cloud and to demonstrate the consistency of the in situ and remote measurements. The spatial and temporal distributions of the aerosol properties are described. Relations between the aerosol surface area concentration *S* (in square micrometers per cubic centimeter) and chlorine monoxide (ClO) concentrations (in parts per trillion by volume) are described for mid-latitude measurements.

The aerosol properties reported here were determined from the output of three instruments flown on the National Aeronautics and Space Administration (NASA) ER-2 high-altitude aircraft in the Airborne Arctic Stratospheric Expedition II (AASE II). The ER-2 Condensation Nucleus Counter (ER-2 CNC) (*1*) measures the concentration of particles in the diameter range from ~0.02 to ~2 μm. The size distributions measured with the focused cavity aerosol spectrometer (FCAS) (Particle Measuring Systems Inc., Boulder, Colorado) typically extend from 0.068 to 3.3 μm (*2*). These highly resolved size spectra extend to the smallest diameters accurately measured in the stratosphere. The forward scattering spectrometer probe (FSSP-300) covers the diameter range from ~0.4 to 20 μm (*3*). The measurements reported here were made between 20 August 1991 (910820) and 26 March 1992 (920326) (Table 1).

Balloon soundings, lidar measurements, and data from the Stratospheric Aerosol and Gas Experiment II (SAGE II) aboard the Earth Radiation Budget Satellite (*4*) show that much of the cloud was above the ER-2 ceiling in August and September 1991. Most of the cloud was within reach of the ER-2 during the high-latitude flights made in October. During the winter of 1991–1992, we made in situ measurements in portions of the mid-latitude cloud having the greatest optical extinctions (Fig. 1) and maximum values of *S*. The fraction of the

Table 1. Analyzed flights from AASE II.

Dates	Latitude range	Number of flights
910820–910917	22°N to 51°N	3
911004–911014	37°N to 90°N	5
911208–920326	22°N to 70°N	15

J. C. Wilson, H. H. Jonsson, C. A. Brock, Department of Engineering, University of Denver, Denver, CO 80208.
D. W. Toohey, Department of Geosciences, University of California, Irvine, CA 92717.
L. M. Avallone, Department of Chemistry, Harvard University, Cambridge, MA 02138.
D. Baumgardner and J. E. Dye, National Center for Atmospheric Research, Box 3000, Boulder, CO 80307.
L. R. Poole and D. C. Woods, National Aeronautics and Space Administration, Langley Research Center, Hampton, VA 23681.
R. J. DeCoursey, M. Osborn, M. C. Pitts, Science Applications International Corporation, Hampton, VA 23666.
K. K. Kelly, National Oceanic and Atmospheric Administration, Aeronomy Lab, 325 Broadway, Boulder, CO 80303.
K. R. Chan, G. V. Ferry, M. Loewenstein, J. R. Podolske, A. Weaver, National Aeronautics and Space Administration, Ames Research Center, Moffett Field, CA 94035.

*To whom correspondence should be addressed.

cloud within reach of the ER-2 increased at northern latitudes. Most of the material resulting from the eruption was below ER-2 ceilings in the polar vortex as a result of the subsidence there, which reduced the altitude of the volcanic cloud.

Features in the size distributions (Fig. 2) reflect physical processes that have been observed and modeled after several eruptions (5). Injected SO_2 is converted to H_2SO_4 in a few months, and the acid vapor condenses on existing particles or forms new particles. New particles in the diameter range from 0.02 to 0.1 μm appeared in the number distribution (Fig. 2B) measured 78 days after the eruption. This peak, referred to as the nuclei mode (6) and containing N_n particles per cubic centimeter, dominates the number distribution. Eight months after the eruption (Fig. 2D), collisions between particles (coagulation) had reduced N_n.

The growth of particles as a result of condensation and coagulation with smaller particles explains the differences in particle size seen in Fig. 2, A and D. Particle size can be conveniently represented by the median surface diameter, D_{sm}, which corresponds to the value of diameter, D_p, that divides the area under the curve in the surface distribution into two equal parts. The value of D_{sm} increased from less than 0.4 μm before the eruption (Fig. 2A) to 1 μm (Fig. 2D). The population of particles seen most clearly in the surface distributions between 0.1 and 2 μm is referred to as the accumulation mode (6) and contains N_a particles per cubic centimeter. Much of the aerosol mass condensing out of the gas phase ultimately accumulates on particles in this mode.

Larger particles containing crustal materials were also injected directly by the eruption and were soon coated by condensing H_2SO_4 (7, 8). Growth of accumulation mode particles at higher altitude and subsequent sedimentation may also supply large particles at the sampled altitude (8). Large particles fall faster than small ones. A mode containing particles with diameters larger than 2 μm dominates the volume distribution in Fig. 2B, but large particles were not encountered at altitudes near 20 km after August. Large particles were seen in the volume distribution at an altitude of 13 km as late as February (Fig. 2C).

The stratospheric aerosol near an altitude of 20 km is often described as having one mode (9–11). This description certainly applies to the preeruption profile above 16.5 km (Fig. 3A) and is reasonably accurate for the posteruption profile (Fig. 3B) above 15 km. At those altitudes, N_n is much smaller than N_a and there are no large particles present. Below those altitudes, the nuclei mode becomes more important in both profiles. The requirement for a source of new particles to maintain the nuclei mode near the tropopause has been noted for the nonvolcanic case (10) and holds for the posteruption profile as well. The size distribution (Fig. 2C) measured near the bottom of the profile shown in Fig. 3B clearly shows a nuclei mode. Aerosol formation just above the tropopause depe

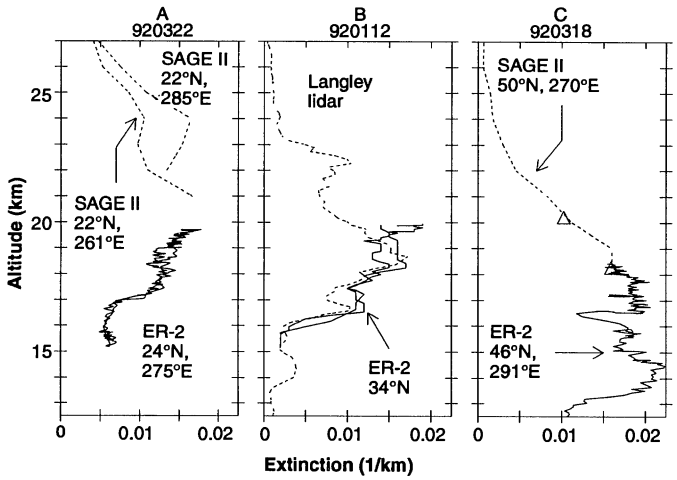

Fig. 1. Profiles of optical extinction determined by SAGE II at a wavelength of 525 nm (**A** and **C**) and by the NASA Langley lidar (**B**) at 694 nm with extinctions calculated from size distribution measurements from the ER-2. Remote measurements (- - - -); ER-2 measurements (—— and triangles). Extinction is a measure of the attenuation of direct sunlight due to scattering and absorption by particles. The extinction equals the inverse of the distance the beam must travel through the aerosol so that the direct beam is reduced by a factor of 1/*e*. The SAGE II profiles terminate when the extinction of the atmosphere is too great to permit an accurate measurement. The ER-2 profile in (B) occurred in air that was thought to have passed over Langley at the time of the lidar measurement.

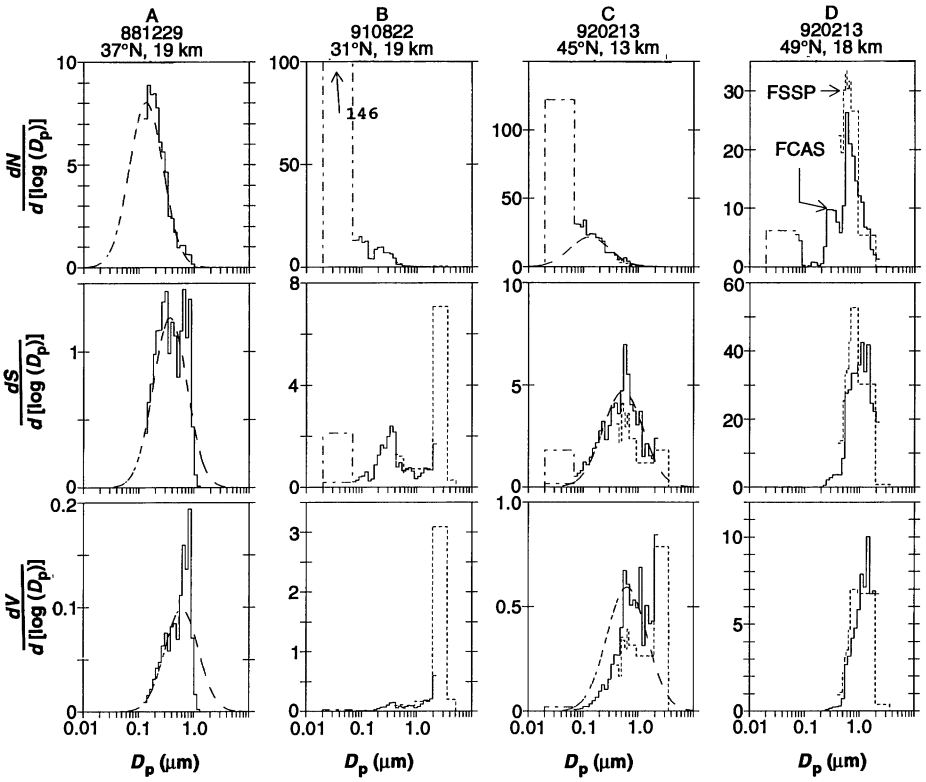

Fig. 2. Aerosol distributions before (**A**) and after (**B** through **D**) the 1991 Mount Pinatubo eruption: number, *N* (particles per cubic centimeter) (top panel); surface, *S* (square micrometers per cubic centimeter) (middle panel); and volume, *V* (cubic micrometers per cubic centimeter) (bottom panel). FCAS (——); FSSP-300 (- - - -); difference between ER-2 CNC and FCAS (— - —); results of lognormal fit to surface distribution (— — —). Surface and volume distributions are calculated from measured number distributions. The upper and lower limits of surface and volume contributed by particles in the range 0.02 to 0.068 μm are shown. Distribution (A) was measured with a passive cavity aerosol spectrometer (*10*).

gases and particles into that region, and this transport is not well understood.

The vertical distribution of the aerosol parameters measured 8 months after the eruption shows that N_n and N_a had returned to near preeruption values. However, S and the H_2SO_4 mass mixing ratio M [in parts per billion by mass (ppbm)] were greatly enhanced (Fig. 3). We found that S varied strongly with latitude at ER-2 cruise altitudes (above the 410 K Θ surface) in the 4 months after the eruption. The minima in S approached nonvolcanic levels, with the larger values of S enhanced by factors reaching 30 (Fig. 4A). Both M and D_{sm} varied from nonvolcanic minima of 0.45 ppbm and 0.3 μm, respectively, to enhanced maxima of 29 ppbm and 0.93 μm. Steep spatial gradients were exhibited by S, M, and D_{sm}.

Later measurements south of the polar vortex showed much less variability at altitudes above the 410 K Θ surface. Strongly enhanced values of S were observed at all latitudes sampled (Fig. 4B). Values of M reached 60 ppbm, and D_{sm} exceeded 1.1 μm in some cases during this period. There was much less variability in S, M, and D_{sm} at this time than in the fall.

Strong horizontal gradients were observed at the edge of the polar vortex, defined as the maximum in wind speed. Increased subsidence inside the vortex lowers the aerosol profile with respect to that observed outside (*12*). The lowering was sufficient to bring cleaner air within reach of the ER-2 inside the vortex. Even in this cleaner air, there was clear spatial inhomogeneity with some strongly enhanced values. At altitudes below the 410 K Θ surface, larger values of S were encountered.

Because of the highly variable aerosol loading observed in the fall months, it was possible to study the effect of S on ClO, a participant in the catalytic cycles by which Cl destroys O_3. In mid-latitude air, the rate of O_3 loss to Cl is proportional to the concentration of ClO. The reaction $N_2O_5 + H_2O \rightarrow 2HNO_3$ is thought to occur on the surfaces of sulfate aerosol, and it is expected to reduce the concentration of NO_2, which, in turn, should permit an increase in ClO (*13*). Models that include this reaction predict more O_3 loss due to Cl in background air and in volcanically enhanced aerosol than do models that exclude it (*14*).

Data from mid-latitude flights in August, September, and October 1991 show that the ratio ClO/Cl_y tends to increase with S [Cl_y is the total amount of inorganic chlorine and is determined from N_2O (*15*)]. A number of factors including latitude, solar zenith angle, and altitude affect ClO concentrations. The data sets used to produce Fig. 5 were screened with the following criteria. The potential temperatures Θ were limited to above 460 K to limit the altitude range. The solar zenith angle was limited to less than 75° to limit the effect of changing light intensity on ClO (*16*). Latitude ranges were limited to 15° bands. Subsets of the data in which aerosol surface and N_2O were correlated with an R^2 of greater than 0.16 were excluded to avoid mistaking the effects of systematic changes of N_2O for the effects of changing S. The positive correlation between ClO/Cl_y and S is consistent with the occurrence of the $N_2O_5 + H_2O$ reaction on sulfate aerosols. Elevated values of ClO/Cl_y were also seen at small values of S (Fig. 5A), indicating that not all the factors affecting the ratio have been controlled in this analysis.

A second heterogeneous reaction, $ClONO_2 + H_2O \rightarrow HOCl + HNO_3$, also occurs on the surfaces of particles; the HOCl that is produced is photolyzed to produce Cl. However, this reaction only occurs on particles that have small mass fractions of sulfuric acid (*14*). Such particles are found at low temperatures, which did not occur in the air parcels analyzed here. To avoid air that had been processed by polar stratospheric clouds, we excluded the winter data near and in the polar vortex from consideration.

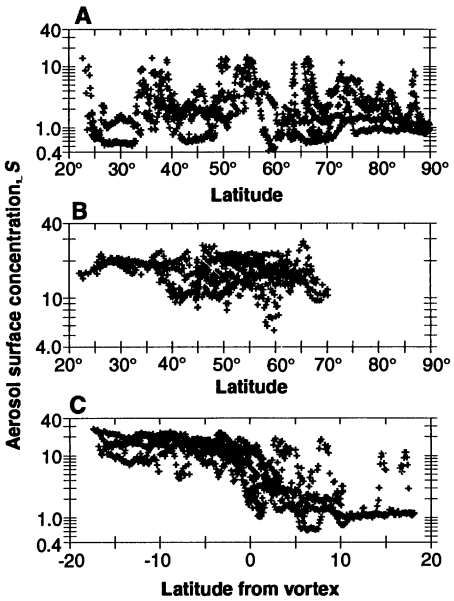

Fig. 4. Aerosol surface area concentration, S (square micrometers per cubic centimeter), plotted against latitude: (**A**) fall 1991; (**B** and **C**) winter 1991–1992. For (A) through (C) Θ >410 K.

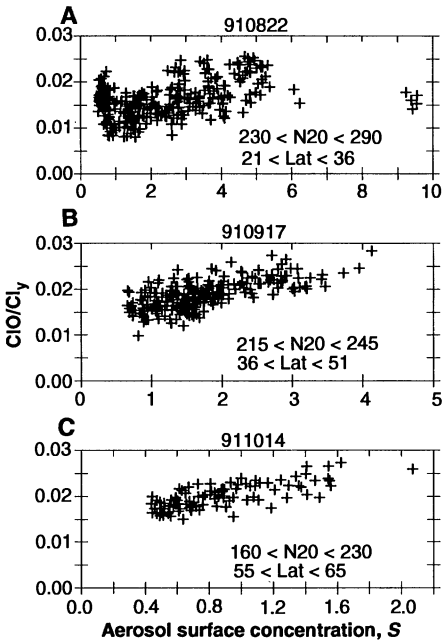

Fig. 5. The ClO/Cl_y ratio plotted against aerosol surface concentration, S (square micrometers per cubic centimeter) for (**A**) August, (**B**) September, and (**C**) October 1991. Screening was done to prevent the effects of changing solar zenith, latitude, altitude, and N_2O from being mistaken for the effects of changes in S.

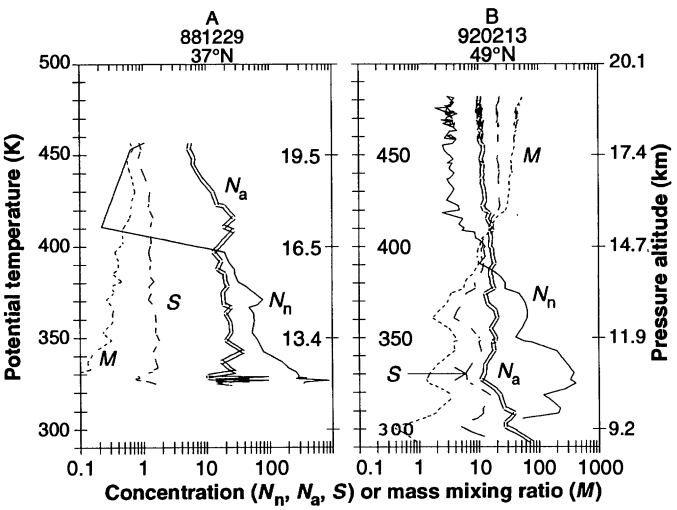

Fig. 3. Aerosol profiles before (**A**) and 8 months after (**B**) the Mount Pinatubo eruption: N_n (particles per cubic centimeter) (——); N_a (particles per cubic centimeter) (═══); M (parts per billion) (- - - -); S (square micrometers per cubic centimeter) (— — —). Right vertical axes are pressure altitude, and left vertical axes are potential temperature (Θ) (*17*).

REFERENCES AND NOTES

1. J. C. Wilson, J. H. Hyun, E. D. Blackshear, *J. Geophys. Res.* **88**, 6781 (1983).
2. The FCAS was calibrated with aerosol having a refractive index very near that of the measured particles. The inlet system (*10*) samples particles from the free stream and transports them to the FCAS for measurement. Sampling artifacts such as anisokinetic sampling and evaporation of water from particles due to heating in sampling and transport are accounted for in the data analysis. It is assumed that the aerosol is a liquid solution of sulfuric acid and water in equilibrium with the ambient water vapor. The reported size distributions reflect ambient conditions and include the water lost as a result of evaporation.
3. D. Baumgardner, J. E. Dye, B. W. Gandrud, R. G. Knollenberg, *J. Geophys. Res.* **97**, 8035 (1992). The FSSP-300 senses particles with minimal disturbance to the free stream and, hence, minimal alteration. Both the FSSP-300 and FCAS measure particles in the diameter range from 0.4 to ~3 μm. Simultaneous FSSP-300 and FCAS measurements of aerosol concentrations in this diameter range typically differ by from a few percent to a factor of 2. This difference is small compared to the dynamic range of aerosol concentrations observed. Measurements made in the volcanic cloud when most particles were of such a size as to be detected by all three instruments were similar.
4. M. P. McCormick and R. E. Veiga, *Geophys. Res. Lett.* **19**, 155 (1992); T. Deshler, D. J. Hofmann, B. J. Johnson, W. R. Rozier, *ibid.*, p. 199; M. J. Post, C. J. Grund, A. O. Langford, M. H. Proffitt, *ibid.*, p. 195.
5. G. J. S. Bluth, S. D. Doiron, C. C. Schnetzler, A. J. Krueger, L. S. Walter, *ibid.*, p. 151; L. A. Capone *et al.*, *ibid.* **10**, 1053 (1983); J. C. Wilson, E. D. Blackshear, J. H. Hyun, *ibid.*, p. 1029; S. A. McKeen, S. C. Liu, C. S. Kiang, *J. Geophys. Res.* **89**, 4873 (1984); D. J. Hofmann and J. M. Rosen, *Science* **222**, 325 (1983); R. P. Turco, R. C. Whitten, O. B. Toon, *Rev. Geophys. Space Phys.* **20**, 233 (1982).
6. K. T. Whitby, *Atmos. Environ.* **12**, 135 (1978). We determined N_a by fitting the surface distributions in Fig. 2 with lognormal functions and converting from the surface parameters to number concentration. We then determined N_n by subtracting N_a from the ER-2 CNC concentration.
7. P. J. Sheridan, R. C. Schnell, D. J. Hofmann, T. Deshler, *Geophys. Res. Lett.* **19**, 203 (1992).
8. V. R. Oberbeck *et al.*, *ibid.* **10**, 1021 (1983).
9. D. J. Hofmann, *Science* **248**, 996 (1990).
10. J. C. Wilson *et al.*, *J. Geophys. Res.* **97**, 7997 (1992).
11. J. L. Gras and J. E. Laby, *ibid.* **86**, 9767 (1981).
12. D. J. Hofmann, J. M. Rosen, J. W. Harder, *ibid.* **93**, 665 (1988); J. C. Wilson *et al.*, *ibid.* **94**, 16437 (1989).
13. M. Mozurkewich and J. G. Calvert, *ibid.* **93**, 15889 (1988); J. M. Van Doren *et al.*, *J. Phys. Chem.* **95**, 1684 (1991); D. R. Hanson and A. R. Ravishankara, *J. Geophys. Res.* **96**, 17307 (1991).
14. J. M. Rodriguez, M. K. W. Ko, N. D. Sze, *Nature* **352**, 134 (1991); D. J. Hofmann and S. Solomon, *J. Geophys. Res.* **94**, 5029 (1989); G. Brasseur and C. Granier, *Science* **257**, 1239 (1992).
15. S. R. Kawa *et al.*, *J. Geophys. Res.* **97**, 7905 (1992).
16. W. H. Brune, D. W. Toohey, S. A. Lloyd, J. G. Anderson, *Geophys. Res. Lett.* **17**, 513 (1990).
17. Potential temperature, Θ, is used as a vertical coordinate in Fig. 3. $\Theta = T(1000/P)^{0.286}$, where P is pressure in millibars and T is temperature in kelvin. In the absence of heat transfer, air parcels move along surfaces of constant Θ.

18. The research done at the University of Denver was supported by NASA Upper Atmosphere Research Program grant NAG 2-458. The suggestions of reviewers and editors are gratefully acknowledged.

1 March 1993; accepted 17 June 1993

Stratospheric Meteorological Conditions in the Arctic Polar Vortex, 1991 to 1992

P. Newman, L. R. Lait, M. Schoeberl, E. R. Nash, K. Kelly, D. W. Fahey, R. Nagatani, D. Toohey, L. Avallone, J. Anderson

Stratospheric meteorological conditions during the Airborne Arctic Stratospheric Expedition II (AASE II) presented excellent observational opportunities from Bangor, Maine, because the polar vortex was located over southeastern Canada for significant periods during the 1991–1992 winter. Temperature analyses showed that nitric acid trihydrates (NAT temperatures below 195 k) should have formed over small regions in early December. The temperatures in the polar vortex warmed beyond NAT temperatures by late January (earlier than normal). Perturbed chemistry was found to be associated with these cold temperatures.

The mechanism responsible for causing large perturbations in Arctic stratospheric chemistry has been established as heterogeneous processes on polar stratospheric clouds (PSCs) (*1*). It has been hypothesized that PSCs consist of various nitric acid hydrates, sulfuric acid aerosols, and water ice particles. These clouds tend to form at temperatures below 195 K (*2*), close to the temperature required for the condensation of NATs (*3*). Water ice particles form at temperatures near 188 K and are large enough to fall out of the stratosphere on short time scales. The settling of these ice particles reduces both water and nitrogen concentrations in the stratosphere (dehydration and denitrification, respectively), further perturbing the stratospheric photochemical balance. In this report, we characterize the thermal structure of the Arctic lower stratosphere during the Northern Hemisphere winter of 1991–1992 (AASE II) and contrast this with the corresponding data for the winter of 1988–1989 (AASE I). We will relate these cold temperatures to PSCs and discuss the impact of PSCs on the polar vortex chemistry during the winter period.

In early December 1991, the polar lower-stratospheric temperatures at the 460 K potential temperature (Θ) surface (*4*) were cold (<205 K), and by late December they had cooled by an additional 10 K (*5*). In early January 1992, the cold temperatures straddled the polar night boundary and were located near the vortex edge (*6*), with a minor warming that raised temperatures above 195 K in late January (Fig. 1). During 1989, the cold temperatures were located mainly in the polar night, well inside of the polar vortex boundary, with a major warming in February 1989 (*7, 8*).

We examined the relation between the 1991–1992 cold temperatures and the perturbed chemistry in the stratosphere by using back trajectories to estimate the coldest temperature experienced by air parcels 10 days before sampling by the National Aeronautics and Space Administration (NASA) ER-2 aircraft (*9*). We then used measured H_2O and derived HNO_3 data (*10*) to estimate the NAT phase transition temperature. High concentrations of chlorine monoxide (ClO) (in excess of 200 parts per trillion) marked air parcels that experienced heterogeneous chemistry on PSCs. The National Meteorological Center (NMC) temperatures observed on the back trajectories (Fig. 2) reveal that (i) at temperatures below the NAT phase transition concentrations of ClO were almost always high, (ii) at temperatures slightly above the phase transition there was some perturbed chemistry (but generally not to the same degree as at those points well below the phase transition), and (iii) at temperatures 6 K higher than the phase transition concentrations of ClO were low. Hence, NMC temperatures, combined with the estimates of NAT phase transitions, provide a conservative technique for inferring the presence of a PSC.

Because these cold temperatures in the NMC fields are linked to the perturbed chemistry observed by the ER-2 [most probably PSCs or the accelerated hydrolysis of chlorine nitrate ($ClONO_2$) at temperatures below 200 K], the ER-2 observations (*10, 11*) can be used to analyze the impact of cold temperatures on the polar

P. Newman, L. R. Lait, M. Schoeberl, National Aeronautics and Space Administration Goddard Space Flight Center, Code 916, Greenbelt, MD 20771.
E. R. Nash, Applied Research Corporation, Landover, MD 20785.
K. Kelly and D. W. Fahey, National Oceanic and Atmospheric Administration Aeronomy Laboratory, 325 Broadway, Boulder, CO 80303.
R. Nagatani, National Meteorological Center Climate Analysis Center, World Weather Building, Washington, DC 20233.
D. Toohey and L. Avallone, Department of Geosciences, Physical Sciences Annex 206, University of California, Irvine, CA 92717.
J. Anderson, Harvard University Atmospheric Research Project, Engineering Science Laboratory, 40 Oxford Street, Cambridge, MA 02138.